Pion double charge exchange on $T=2$ nuclei in the $\Delta_{3/2,3/2}$ resonance region

P. A. Seidl,[2] M. A. Bryan,[6] M. Burlein,[5,*] G. R. Burleson,[4] Kalvir S. Dhuga,[4,†] H. T. Fortune,[5] R. Gilman,[5,1,‡] S. J. Greene,[3] M. A. Machuca,[6] C. Fred Moore,[6] S. Mordechai,[6,§] C. L. Morris,[3] D. S. Oakley,[6,**] M. A. Plum,[3] G. Rai,[2] M. J. Smithson,[6,††] Z. F. Wang,[3] D. L. Watson,[3,7] and J. D. Zumbro,[5,‡‡]

[1] *Argonne National Laboratory, Argonne, Illinois 60439*
[2] *Lawrence Berkeley Laboratory, Berkeley, California 94720*
[3] *Los Alamos National Laboratory, Los Alamos, New Mexico 87545*
[4] *New Mexico State University, Las Cruces, New Mexico 88003*
[5] *University of Pennsylvania, Philadelphia, Pennsylvania 19104*
[6] *University of Texas at Austin, Austin, Texas 78712-1081*
[7] *University of York, York YO1 5DD, United Kingdom*

(Received 25 July 1990)

We present cross sections for the reactions ^{44}Ca,^{56}Fe (π^+,π^-)leading to the residual ground states and double-isobaric-analog states (DIAS) for incident pion energies from 100 to 300 MeV. Data include both angular distributions and 5° excitation functions. Ground-state cross sections were also obtained from the ^{12}C and ^{16}O contaminants in the ^{44}Ca target. The DIAS data are compared to known systematics and to theoretical predictions. Some features of the data are reproduced by the theoretical predictions, but major discrepancies exist.

I. INTRODUCTION

The (π^+,π^-) double-charge-exchange (DCX) reaction is a sensitive probe of two-nucleon effects and structure, because it is a two-nucleon process in lowest order. Untangling structure information from reaction-mechanism effects has, however, proven difficult. As yet, no microscopic theory exists which explains transitions to both residual ground states and double-isobaric-analog states (DIAS) over a large range of incident energies. Near 300-MeV incident kinetic energy, lowest-order theories appear consistent with the data. Higher-order processes are relatively weak (at least at forward angles) and the reaction is more sensitive to the gross numbers of nucleons rather than to the fine details of nuclear structure.[1-5] At low energies, below about 100 MeV, it has been shown with several complimentary theoretical approaches[6-8] that simple shell-model effects are an important ingredient in understanding the data. At $\Delta_{3/2,3/2}$ resonance energies, second-order reaction mechanism effects are large but poorly understood.[9-11] Cross sections for nonanalog residual ground states are large and can be understood as arising from a delta-nucleon interaction mechanism.[12,13] For DIAS residual states, a number of reaction mechanisms seem to be important, and the only successful theories are certain phenomenological models[9,11] in which the first- and second-order pi-nucleon optical potentials interfere to produce the forward minima seen[3,14,15] in the data for DIAS on $T = 1$ nuclei. Since the second-order optical potential is isospin dependent,[9,10] one expects an isospin dependence in resonance-energy DIAS angular distribution shapes. This prediction has not been tested experimentally until this work.

Recently there has been much interest in measurements on fp-shell nuclei. With certain models of the nuclear structure, analytic expressions can be derived for ratios of the cross sections for isotopes within the same shell.[7] Transitions to residual ground states and DIAS in fp-shell isotopes require two amplitudes, which are related to the long- and short-range parts of the interaction. The amplitudes have been extracted[5,7,16] with fits of both low-energy data and data at 292 MeV. It appears that, for $T > 1$ nuclei, the strength of the short-range term is lessened relative to that of the long-range uncorrelated part of the amplitude, and the minimum in the angular distribution should move to larger angles. This model has not, however, been studied in detail in the resonance region.

In addition, there is an older class of two-amplitude models[17] developed to explain the forward minima seen in the $T = 1$ angular distributions. In these models, the DCX amplitude is divided into a $\Delta T = 0$ analog component and a $\Delta T = 2$ nonanalog component. For $T = 1$ targets, both amplitudes contribute to the residual ground state, g.s., which is also the DIAS, producing the known interference. For a $T = 2$ target, the $\Delta T = 2$

TABLE I. Target properties. Two ^{56}Fe targets were used.

Property	^{44}Ca	^{56}Fe
Areal density (g/cm^2)	1.5	2.4 / 1.2
Chemical form	$^{44}CaCO_3$ with polyethylene binder	1010 steel
Chemical purity (%)	30	95
Isotopic purity (%)	98.4 (enriched)	91.2 (natural)
Experimental resolution (MeV)	0.84	1.00 / 0.64
Ground state Q value (MeV)	−2.9	−5.7
DIAS excitation energy (MeV)	9.0±0.2	9.90±0.05

nonanalog strength leads primarily to the g.s. The DIAS results almost solely from the analog strength, and the angular distribution should resemble first-order calculations, rather than showing interference effects.

In this paper, we present measurements of ^{44}Ca,^{56}Fe (π^+,π^-) to the residual ground states and DIAS from 100 to 300 MeV. We present the first $T > 1$ angular distributions measured at and above resonance energies. Although naively we might expect deep forward minima for $T = 2$ DIAS angular distributions, as are observed in those on $T = 1$ targets, there are several reasons to expect shape changes, and these data test the predictions.

II. EXPERIMENTAL DETAILS

The measurements were made at the Clinton P. Anderson Meson Physics Facility (LAMPF) with the Energetic Pion Channel and Spectrometer (EPICS). Descriptions of the channel, spectrometer, and modifications for forward angle DCX measurements have been presented elsewhere.[2,14] We note that the nonpion background is reduced to a negligible level with a system that includes a Cherenkov detector, time-of-flight measurements, a stack of scintillators and carbon slabs for rejecting muons, and angle check cuts to exclude pions decaying in flight. Target properties are shown in Table I. Pion DCX background does occur from contaminants in the targets, but the contaminants are either isotopes present in small amounts, such as other Fe isotopes, or isotopes with much more negative Q values, such as ^{12}C ($Q = -32.0$ MeV) or ^{16}O ($Q = -28.4$ MeV).

The DCX data were normalized by measuring yields for ^{1}H $(\pi^+,\pi^+)^1$H at $\theta = 40°$, and comparing them to cross sections calculated from π-nucleon phase shifts.[18] An angular distribution for ^{1}H $(\pi^+,\pi^+)^1$H showed that any angle-dependent systematic errors are less than 3%. Cross sections were extracted with a line-shape fitting code that uses the CERN MINUIT optimization package.[19] The fitted line shape was a Landau distribution folded with a Gaussian required to fit elastic scattering spectra, thus taking into account both instrumental resolution and straggling in the targets. The resulting cross sections are given in Tables II, III, and IV. For the ^{56}Ni(g.s.) at 292 MeV, only upper limits of similar magnitude were obtained at all angles, and we report only the limit at 5°. The systematic uncertainty in the absolute cross sections is about 10%.

Some spectra are shown in Fig. 1. Due to the relatively poor signal-to-noise ratio at lower energies[20] and at larger angles, several sensitivity checks were performed on the fitting procedures. In particular, different line shapes (all required to fit elastic scattering), background shapes (polynomial and exponential parameterizations), numbers of peaks, and statistics (χ^2 and Poisson[21]) were all tested. The systematic variations with model were found to be typically half the quoted uncertainty. For example, for the ^{56}Fe 180-MeV angular distribution, the most prominent model dependence is the choice of number of peaks in the spectrum. Three peaks with an exponential background fit the data well (reduced χ^2 is about 1). Including additional small, but poorly determined, peaks reduces the average level of the background curve, and increases the number of DIAS counts. Removing all non-DIAS excited states in the fit to these data would decrease cross sections by about 10%.

TABLE II. ^{56}Fe$(\pi^+,\pi^-)^{56}$Ni(DIAS) cross sections from this work.

T_π (MeV)	θ (deg)	$d\sigma/d\Omega$ (nb/sr)
100	5	74 ± 30[a]
120	5	55 ± 21[a]
164	5	34± 12
164	10	30 ± 11
180	5	72 ± 13[a]
180	5	68 ± 13
180	10	35 ± 8
180	15	22 ± 4
180	20	19 ± 6
180	25	11 ± 5
180	30	< 10
230	5	172 ± 43[a]
292	5	413 ± 77[a]
292	5	234 ± 40
292	10	70 ± 20
292	15	28 ± 12
292	20	55 ± 18
292	25	47 ± 15
292	30	21 ± 11
292	35	13 ± 10

[a] These cross sections result from a reanalysis of earlier data.[4]

TABLE III. $^{56}Fe(\pi^+,\pi^-)^{56}Ni$(g.s.) cross sections from this work.

T_π (MeV)	θ (deg)	$d\sigma/d\Omega$ (nb/sr)
100	5	< 28[a]
120	5	61 ± 20[a]
164	5	33± 9
164	10	6± 6
180	5	22 ± 8[a]
180	5	19± 6
180	10	7± 3
180	15	4± 2
180	20	< 1
180	25	7± 3
180	30	5± 2
230	5	< 8[a]
292	5	< 11[a,b]

[a] These cross sections result from a reanalysis of earlier data.[4]
[b] Upper limits at larger angles at 292 MeV are slightly smaller than at 5°.

III. DISCUSSION

In general, the overlap of the present data with previous results is good. Cross sections were extracted for the ^{12}C (π^+,π^-) and ^{16}O (π^+,π^-) reactions with the $^{44}CaCO_3$ target, and the agreement with previous measurements[22–24] is satisfactory despite large acceptance corrections. The agreement of the ^{56}Fe data with our previous work[20] is also good (see Fig. 2). Some of the ^{56}Fe excitation function data (see Table II and III) result from a reanalysis of data previously presented.[4,25] (On average, the differences are less than an error bar, consistent with the remarks above.) The extracted DIAS excitation energy for ^{56}Fe given in Table I (9.90 ± 0.05 MeV) is more reliable than our previous value[20] due to more precise energy calibration procedures and the improved analysis, and is in better agreement with determinations from $^{54}Fe(^3He,n)^{56}Ni$ and $^{58}Ni(p,t)^{56}Ni$, which find $E_x \simeq 9.97$ MeV.[26]

The 5° excitation-function data for ^{44}Ca and ^{56}Fe, shown in Fig. 2, follow the systematics of $T = 1$ nuclei.[2,3] For energies above 170 MeV the cross section increases with energy. In the 100–170 MeV energy range, different $T = 1$ nuclei exhibit different patterns, but in the present work the cross sections at these energies are not well enough determined to distinguish between the different behaviors. Ground-state transitions are peaked near 160 MeV as seen with other nonanalog transitions.[12,22]

The ^{56}Fe angular distributions are compared to theory in Fig. 3. At 292 MeV, the reaction mechanism is believed to be simple and understood, due to the apparent simplicity of the data.[2–5] First-order theories calculate sequential charge exchange through the intermediate single analog state, and qualitatively reproduce the data. We see, however, that the first-order theory tends to underpredict the cross sections at the larger angles relative

TABLE IV. Other (π^+,π^-) cross sections from this work.

Reaction	T_π (MeV)	θ (deg)	$d\sigma/d\Omega$ (nb/sr)
$^{12}C(\pi^+,\pi^-)^{12}O$(g.s.)	180	5	383 ± 75
	210	5	262 ± 48
	260	5	88 ± 58
	292	5	60 ± 31
$^{16}O(\pi^+,\pi^-)^{16}Ne$(g.s.)	140	5	492 ±160
	164	5	439 ± 72
	180	5	249 ± 71
	210	5	218 ± 53
	260	5	260 ± 93
	292	5	215 ± 52
$^{44}Ca(\pi^+,\pi^-)^{44}Ti$(g.s.)	120	5	292 ± 90
	140	5	281 ± 58
	164	5	139 ± 24
	180	5	102 ± 34
	180	10	65 ± 29
	210	5	< 41
	260	5	< 130
	292	5	< 76
$^{44}Ca(\pi^+,\pi^-)^{44}Ti$(DIAS)	120	5	87 ± 69
	140	5	61 ± 34
	164	5	40 ± 21
	180	5	190 ± 47
	180	10	168 ± 47
	210	5	300 ± 69
	260	5	1013 ± 188
	292	5	587 ± 106

to those at forward angles. This behavior can also be seen for ^{14}C, ^{18}O, and ^{26}Mg at 292 MeV.[2,3] In general, it is difficult to increase the predicted cross section at larger momentum transfers. The addition of short-range correlations in some models[12,13] decreases the predicted cross sections at larger angles relative to those at smaller angles. It is difficult to assess whether this systematic discrepancy between data and theory results from problems in the optical potential or from the contribution of some short-range phenomenon.

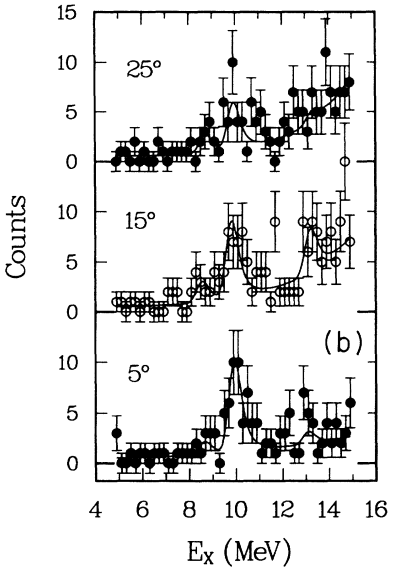

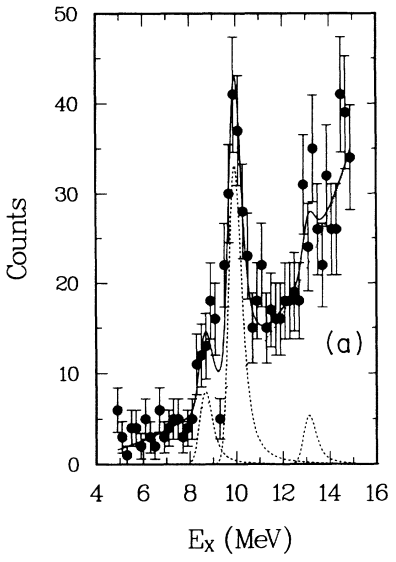

FIG. 1. Examples of fits to the excitation energy spectra for ^{56}Fe(π^+,π^-) at 180 MeV. In (a), the sum of data at all angles is shown. In (b), spectra at three angles are shown. The error bars (1σ) represent the statistical uncertainty of the data. The fit to the data is shown as a solid line. In (a), the dashed lines are the three peaks and the dotted line is the exponential background used to parametrize the data. The DIAS is at 9.90 ± 0.05 MeV; the identity of the peaks 1.3 MeV below and 3.2 MeV above the DIAS is ambiguous. The spectrum has not been corrected for spectrometer acceptance as a function of excitation energy (a 3% effect).

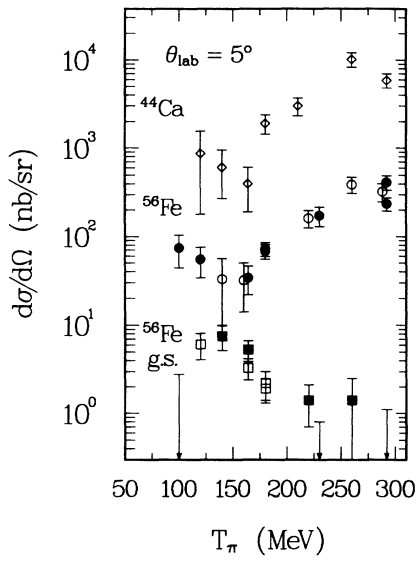

FIG. 2. Excitation functions at $\theta = 5°$ for ^{44}Ca(π^+,π^-) DIAS (diamonds, multiplied by 10), ^{56}Fe(π^+,π^-) DIAS (solid circles from this work and open circles from earlier work[20]), and ^{56}Fe(π^+,π^-) ^{56}Ni(g.s.) (solid squares from this work, open squares from earlier work,[20] multiplied by 0.1). The old ^{56}Fe(π^+,π^-) DIAS data at 164 and 292 MeV has been offset slightly for display purposes.

The ^{56}Fe data at 180 MeV resemble none of the predictions. One might naively expect the data to exhibit a deep forward minimum, as has been observed in $T = 1$ nuclei, and as represented by the prediction for ^{54}Fe shown in Fig. 3. Alternatively, as in certain interference models, one might expect the DIAS to be simply diffractive, as are $T = 0$ to $T = 2$ transitions at this energy,[22,23] as shown by the 180-MeV first-order curve in Fig. 3. For another possibility, one might expect the isospin dependence of the second-order optical potential to change the angular distribution shape, as shown in the second-order curve in Fig. 3. The data do not support any of these expectations.

Additional points at 10° and 180 MeV for ^{44}Ca and at 10° and 164 MeV for ^{56}Fe indicate that the cross sections fall off more slowly with angle than one expects based on measurements for $T = 1$ or $T = 0$ nuclei, but the statistics are poor. Attempts were made to make additional measurements at larger angles at 164 and 180 MeV for ^{44}Ca, and at 164 MeV for ^{56}Fe, but because of limited statistics and a small signal-to-noise ratio it was impossible to extract reliable cross sections.

In interpreting the disagreement between the second-order isospin-dependent theory and the data, it is also important to recall that second-order ρ^2 parameters are energy dependent, and the calculations presented use 164-MeV parameters at 180 MeV. There are insufficient data at 180 MeV to repeat the fitting procedures of Greene *et al.*,[11] but we have estimated changes in the parameters

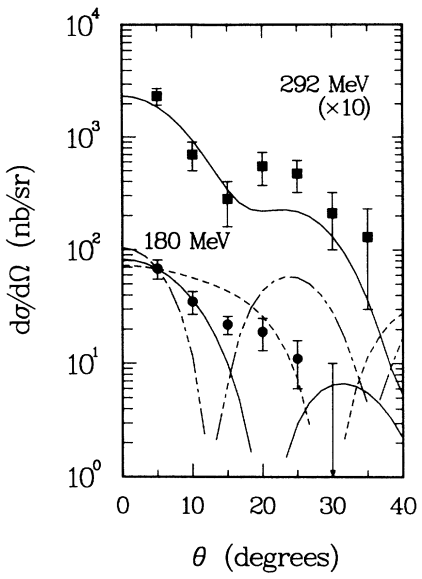

FIG. 3. Angular distributions at 292 (squares) and 180 MeV (circles) for ^{56}Fe(π^+,π^-) DIAS. The ^{56}Fe data at 292 MeV and the calculation have been multiplied by 10. The calculations shown were done with the code PIESDEX,[10] and include a first-order calculation (solid curve), a second-order calculation (dashed curve), and a second-order calculation for the $T = 1$ nucleus ^{54}Fe (long-short dashed curve). The first-order calculation at 292 MeV has been normalized to the three small-angle data points. The calculations at 180 MeV have been normalized to the datum at 5°.

based on fits at 230 MeV,[27,28] and find no major change in the predicted angular-distribution shape.

We conclude that the present data do not support any of the standard DCX models for the resonance energy region. The 180-MeV ^{56}Fe angular distribution most closely resembles that for ^{14}C (π^+,π^-) DIAS at 164 MeV,[3] the shape of which has not been adequately explained. While the quality of the data is not sufficient to completely rule out any of the models, it does indicate the need for improved reaction models at both resonance and higher energies.

The state observed just below the DIAS for ^{56}Fe may be related to $T_<$ states observed in other nuclei.[29] In the present data at 180 MeV, one of the non-DIAS states used had $E_x = E_x(\text{DIAS}) - 1.3 \pm 0.2$ MeV, in agreement with these observations. The cross sections for this state were about 9 ± 5 nb/sr at each angle. Thus, it is difficult to make strong conclusions about the shape of the angular distribution.

IV. CONCLUSION

We have measured angular distributions and excitation functions for (π^+,π^-) on two $T = 2$ nuclei. The excitation functions are consistent with expectations based on systematics from other nuclei. Angular distributions at 292 MeV systematically exceed first-order predictions at the larger angles. The ^{56}Fe angular distribution at 180 MeV is not in good agreement with any of the three predictions for its shape. These data indicate a need for both improved reaction models at energies on and above the $\Delta_{3/2,3/2}$ resonance and more precise experiments.

ACKNOWLEDGMENTS

This work was supported in part by the U.S. Department of Energy, the Robert A. Welch Foundation, and the National Science Foundation. Lawrence Berkeley Laboratory was supported by the U.S. Department of Energy under Contract No. DE-AC03-76SF00098. Argonne National Laboratory is supported by the U.S. Department of Energy Nuclear Physics Division under Contract No. W-31-109-ENG-38.

*Present address: Institute for Defense Analysis, Alexandria, VA 22311-1772.
†Present address: George Washington University, Washington, D.C. 20052.
‡Present address: Rutgers, The State University of New Jersey, P. O. Box 849, Piscataway, NJ 08855.
§Permanent address: Ben Gurion University of the Negev, Beer-Sheva, Israel.
**Present address: Lewis and Clark College, Portland, OR 97219.
††Present address: NSF, SERC, Daresbury Laboratory, Sheshire WA4 4AD, UK.
‡‡Present address: Massachusetts Institute of Technology, Bates Linear Accelerator, Middleton, MA 01949.

[1] G. A. Miller, Phys. Rev. C **24**, 221 (1981).
[2] S. J. Greene *et al.*, Phys. Rev. C **25**, 927 (1982).
[3] Peter A. Seidl *et al.*, Phys. Rev. C **30**, 973 (1984).
[4] R. Gilman *et al.*, Phys. Rev. C **35**, 1334 (1987).
[5] J. D. Zumbro *et al.*, Phys. Rev. C **36**, 1479 (1987).
[6] N. Auerbach, W. R. Gibbs, and E. Piasetzky, Phys. Rev. Lett. **59**, 107 (1987).
[7] N. Auerbach, W. R. Gibbs, Joseph N. Ginocchio, and W. B. Kaufmann, Phys. Rev. C **38**, 1277 (1988).
[8] M. Bleszynski and R. J. Glauber, Phys. Rev. C **36**, 681 (1987); and E. Bleszynski, M. Bleszynski, and R. J. Glauber, Phys. Rev. Lett. **60**, 1483 (1988).
[9] L. C. Liu, Phys. Rev. C **27**, 1611 (1983).
[10] M. B. Johnson and E. R. Siciliano, Phys. Rev. C **27**, 730 (1983); **27**, 1647 (1983).
[11] S. J. Greene *et al.*, Phys. Rev. C **30**, 2003 (1984).
[12] R. Gilman *et al.*, Phys. Rev. C **34**, 1895 (1986).
[13] A. Wirzba *et al.*, Phys. Rev. C **40**, 2745 (1989).
[14] S. J. Greene *et al.*, Phys. Lett. **88B**, 62 (1979).
[15] K. K. Seth *et al.*, Phys. Rev. Lett. **43**, 1574 (1979); **45**, 147(E) (1980).
[16] Z. Weinfeld *et al.*, Phys. Rev. C **37**, 902 (1988).
[17] S. J. Greene *al.*, Phys. Rev. C **25**, 924 (1982); and R.

Gilman *et al.*, Nucl. Phys. **A432**, 610 (1985).
[18]G. Rowe, M. Salomon, and R. H. Landau, Phys. Rev. C **18**, 584 (1978).
[19]F. James and M. Roos, Comput. Phys. Commun. **10**, 343 (1975).
[20]Peter A. Seidl *et al.*, Phys. Rev. Lett. **50**, 1106 (1983).
[21]S. Wood, Ph.D. thesis, Massachusetts Institute of Technology (1984), also available as Los Alamos National Laboraotory Report LA-9932-T (1984).
[22]L. Bland *et al.*, Phys. Lett. **128B**, 157 (1983).
[23]S. J. Greene *et al.*, Phys. Rev. C **27**, 2375 (1983).
[24]R. Gilman *et al.*, Phys. Rev. C **29**, 2395 (1984).
[25]H. T. Fortune, *et al.*, Phys. Rev. C **35**, 1151 (1987).
[26]D. Evers *et al.*, Nucl. Phys. **A198**, 268 (1972); and H. Nann and W. Benenson, Phys. Rev. C **10** 1880 (1974).
[27]R. Gilman, dissertation, University of Pennsylvania (1985).
[28]R. Gilman, M. B. Johnson, P. A. Seidl, and E. R. Siciliano (unpublished).
[29]C. Fred Moore *et al.*, Bull. Am. Phys. Soc. **35**, 947 (1990).